Nanoscale

Accepted Manuscript

This article can be cited before page numbers have been issued, to do this please use: Z. Szakács, T. Mészáros, M. I. De Jonge and R. E. Gyurcsányi, *Nanoscale*, 2018, DOI: 10.1039/C8NR01310A.

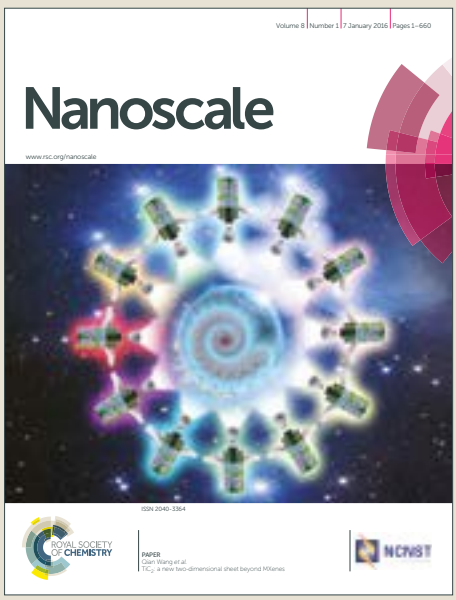

ROYAL SOCIETY OF CHEMISTRY

rsc.li/nanoscale

Nanoscale

View Article Online
DOI: 10.1039/C8NR01310A

ARTICLE

Selective counting and sizing of single virus particles using fluorescent aptamer-based nanoparticle tracking analysis

Zoltán Szakács[a], Tamás Mészáros[b], Marien I. de Jonge[c], Róbert E. Gyurcsányi[a*]

Received 00th January 20xx,
Accepted 00th January 20xx

DOI: 10.1039/x0xx00000x

www.rsc.org/

Detection and counting of single virus particle in liquid samples is largely limited to narrow size distribution viruses and purified formulations. To address these limitations here we propose a calibration-free method that enables concurrently the selective recognition, counting and sizing of virus particles as demonstrated through the detection of human respiratory syncytial virus (RSV), an enveloped virus with broad size distribution, in throat swab samples. RSV viruses were selectively labeled through their attachment glycoproteins (G) with fluorescent aptamers, which further enabled their identification, sizing and counting at single particle level by fluorescent nanoparticle tracking analysis. The proposed approach seems to be generally applicable to virus detection and quantification. Moreover, it could be successfully applied to detect single RSV particles in diluted throat swab samples of diagnostic relevance. Since the selective recognition is associated with the sizing of each detected particle the method enables to discriminate between viral elements linked to the virus as well as between various virus forms and associations.

Introduction

Viruses can be detected either directly or indirectly through the host immune response (e.g. detection of virus-specific antibodies generated in response to the infection).[1] Direct detection certainly prevail to characterize and standardize virus preparations, but are also used for medical diagnostics because it enables genotyping and is more specific than the measurement of host immune responses, e.g. are not restricted by seroconversion times, co-morbidities or treatments.[1] However, the majority of direct detection methodologies target only a single component of the virus, i.e., characteristic nucleic acids and proteins even though virus pathogenesis involves whole virus particles.[2] Therefore, the interpretation of the results may be complicated if the detected viral elements are not linked to intact viral particles but originate from disintegrated viruses or contaminations. A major step in discriminating between the free and virus integrated proteins was made by introducing a dedicated flow cytometry technique[3] based on the concomitant detection of stained viral proteins and nucleic acids, which increases the likelihood of detecting viral components integrated in virus particles. However, in this respect the most comforting would be if the selective detection of particular virus components is associated with the size of the measured entity as well. Virus sizing in the submicron range has been demonstrated with a wide range of techniques including electron microscopy,[4] atomic force microscopy,[5] various light scattering[6, 7] and interferometric techniques,[8] nanoparticle tracking analysis[9, 10] and resistive pulse sensing.[11-13] These techniques if used self-standing are able to size and in some cases even count viruses in properly purified samples such as vaccines, but even their excellent size resolution may not be sufficient to unambiguously identify and quantify viruses in complex biological samples. Therefore, attempts have been made to combine high resolution sizing with specific detection of a viral component mainly by antibodies raised against viral coat proteins to selectively detect virus particles. Techniques capable to detect and count single virus particles in liquids were realized both in heterogeneous and homogeneous formats. Thus surface-immobilized antibodies could be used to capture viruses in predefined spots to be consecutively revealed by AFM imaging[5]. Alternatively, antibodies were added to the sample to selectively increase the size of the viruses that could be detected by resistive pulse sensing.[14] However, despite the maturity of single virus detection methodologies these are still largely limited to purified virus formulations. Moreover, detection methods that are relying, at least partially, on the size of the particles are mostly targeting viruses of well-defined size and difficulties are foreseen if applied for viruses that feature an inherently broad size distribution. Therefore, we were interested to address these limitations by developing a fluorescent nanoparticle tracking analysis methodology that enables the selective detection and counting of single viruses with broad size distribution.

[a] MTA-BME Lendület Chemical Nanosensors Research Group, Department of Inorganic and Analytical Chemistry, Budapest University of Technology and Economics, Szt. Gellert tér 4, H-1111 Budapest, Hungary
E-mail: robertgy@mail.bme.hu
[b] Department of Medical Chemistry, Molecular Biology and Pathobiochemistry, Semmelweis University, Budapest, Hungary.
[c] Section Pediatric Infectious Diseases, Laboratory of Medical Immunology, Radboud University Medical Center, Nijmegen, Netherlands
Electronic Supplementary Information (ESI) available: size distribution of virus formulation in light scattering mode, snapshots of NTA measurements, fluorescence quenching and competition experiments. See DOI: 10.1039/x0xx00000x

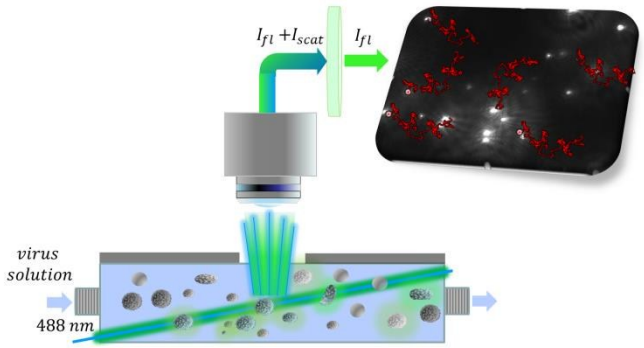

Scheme 1. Schematic of the selective virus sizing and counting by fluorescent nanoparticle tracking. The RSV containing sample incubated with fluorescently labeled aptamer is flown through the thin layer cell illuminated by a 488 nm laser beam. Using a cut-off filter of 495 nm the scattered light is removed and solely the fluorescently labeled virus particles are tracked (red lines). The speed of their motion provides the equivalent diameter of the viruses while the virus count is given by the average number of virus particles detected in the sensing volume.

Nanoparticle tracking analysis (NTA) was introduced as a general method to size and count biological and synthetic nanoparticles in solutions by taking advantage of their light scattering properties.[15-17] The motion of individual nanoparticles is tracked to provide their diffusion coefficient that is further used to calculate their size by Stokes-Einstein equation. Furthermore, nanoparticles can be tracked also by their fluorescence if adequate wavelength excitation lasers and emission filters are applied. Considering this possibility, we hypothesized that adding fluorescently labeled receptors, selective for a surface exposed viral protein, the fluorescent receptor concentration will locally increase around the virus in a sufficient extent to enable its differentiation from the fluorescent background. Accordingly, the virus particles can be identified as fluorescent particles, sized and quantified (Scheme 1). Accordingly, the virus particles can be identified as fluorescent particles, sized and quantified (Scheme 1). Currently, there is strong interest for synthetic receptors for viruses as alternatives to antibodies[1, 18] due to their better stability and versatility in terms of custom chemical modification. Therefore, for the fluorescent detection of virus particles we took advantage of monovalent fluorescently labeled aptamers to rule out virus aggregation. For proof of concept we used respiratory syncytial virus A2 (RSV), an enveloped virus that shows not only a very broad size distribution (ca. 100 -1000 nm)[19] but also variation in shape that includes spherical and filamentous particles.[20] RSV is one of the most common pathogens to cause lower respiratory tract infections that affects all age groups but most severely children younger than 2 years of age as well as elderly and immunocompromised patients. These patients may develop complications and it was estimated that RSV is responsible for up to 35% of pneumonia cases.[21] Given the high diagnostic relevance of RSV detection[22] we explored the application of the single virus detection methodology in throat swab-based samples.

Experimental section

View Article Online
DOI: 10.1039/C8NR01310A

Chemicals and reagents

DNA aptamers labelled with Alexa Fluor 488 at their 5'-ends were custom synthetized by Sigma-Aldrich and formulated as 100 µM solutions in pH=8.0 Tris-EDTA buffer. The variable 30-mer nucleotide regions of the RSV aptamers were flanked by two constant (16-mer) sequences 5' -TAG GGA AG AGA AGG ACA TAT GAT-30 N- TTGACTAGTACATGACCACTTGA-3' (TCC ATA TCG TTT AGC GTA CGG TGG CAG TCT (B10) ; ACC CGT CGG ACT CGG CCA TAA ATT AAA GGC (E6); GTG TCC GTT CTT ATT GGC GGC TCC CAA TGT (E10), TCA TTA GGT GAG TGT CCG TTC TAC ACT ATA (E11); AGT GCG GTG AGC CGT CGG ACA TAC AAA TAC (H8)). As control a random 76-mer DNA sequence (randomDNA) was used (5' –ATC CAG AGT GAC GCA GCA TAT TTC GAC CTT CTA CCT TTG ATT TTT GTG GTC CTC AGT GTG GAC ACG GTG GCT TAG T- 3'). All solutions were prepared or diluted with a pH=7.4 phosphate buffered saline (PBS, P4417, Sigma-Aldrich). To prepare solutions for the NTA experiments the PBS was filtered through 50 nm pore diameter polycarbonate membranes (Osmonics Inc.). FITC labelled anti-respiratory syncytial virus polyclonal antibody (FITC-antiRSV, ab156657) and FITC-labeled anti-nucleoprotein (FITC-ab25849) was purchased from Abcam. Human rhinovirus (HRV) was kindly provided by Kjerstin Lanke (Department of Medical Microbiology, Radboud Medical University).

RSV culturing and formulation

For RSV cultivation RSV A2 infected HeLa cells were used as described in detail previously.[23] The extraction and purification of the RSV followed a previously reported standard procedure.[23, 24] In brief, the cell suspension was subjected to a first centrifugation step of 1800×g for 10 min to remove the rough cell debris, followed by ultracentrifugation over a 30% sucrose layer at 72 000×g for 1.5h. Titration on HeLa cells followed by a permeabilization and fixation step using Perm/Fix buffers (Becton Dickinson). The cells were incubated with FITC-ab25849 for 30min on ice washed with Perm/Wash buffers (Becton Dickinson) and measured on the flow-cytometer (LSR II, Becton Dickinson). The concentration of infectious particles (plaque forming unit equivalents, PFUe) was determined as the number of positive cells per volume. For laboratory use the RSV A2 was inactivated by incubation with β-propiolactone (0.025%) under continuous slow shaking at 4 °C for 16 h.[25] The excess of the reagent was left to hydrolyse for 4 h by increasing the temperature to 37 °C and the resulted formulation was stored at −80 °C.

Throat swab sample collection

Throat swabs were attained from healthy volunteers with medical swab sticks (Meus S.r.L). The swabs were immediately soaked in 2 mL PBS (pH=7.4; 1.37 M NaCl, 27 mM KCl, 20 mM KH_2PO4, 100 mM Na_2HPO_4), vortexed, and then centrifuged at room temperature (19 060xg) for 2 min to transfer the throat sample from the swab into the centrifuge tube. The collected liquid was stored at -20°C.

NTA experiments

The NTA experiments were performed using a NanoSight LM10-HS instrument (Malvern) equipped with a 488 nm laser light source and a sCMOS camera (Hamamatsu Photonics) triggered by the laser. In fluorescence mode a 495 nm cut-off filter was used to eliminate the scattered light. Samples of 200-500 µl were flown through the thin layer cell at 6.5 µL/min flow rate using a syringe pump (Harvard Apparatus). The particle tracks were recorded and analysed by NanoSight NTA 2.3 software package. Of note, the NTA software automatically corrects the random particle motion with the unidirectional movement generated by the sample flow. The particle concentrations were calculated as the average of either at least 5 one-minute measurements or at least 50 particle tracks The throat swab samples were diluted 10-fold and spiked with various RSV concentrations. The samples were further centrifuged at 2500×g for 15 min to remove large size debris and 800 µL aliquots were used for each NTA measurement. The different RSV samples, both formulated in PBS and in diluted throat swab samples, were fluorescently labelled with 25 nM AlexaFluor488-aptamer conjugates (or 25 nM FITC-antiRSV antibody) and subjected to NTA detection in fluorescence mode without separation.

Fluorescence and fluorescence polarization measurements

The fluorescence emission spectra were measured on a Perkin Elmer LS50B luminescence spectrometer. To this end samples were introduced in fluorescence microcuvettes (105.251 QS Hellma) and excited at 490 nm. A 510 nm cut-off filter was used to avoid the detection of scattered light from the throat swab samples. Fluorescence polarization (FP) experiments were performed using a BioTek Synergy 2 microplate reader equipped with a xenon flash lamp and a polarizer set using a 485/20 nm bandpass filter for excitation, a 528/20 nm bandpass filter for emission and 510 nm dichroic mirror. During FP a plane polarized light is used to excite the fluorescent aptamers with the emitted fluorescent light detected in the same plane ($I_{||}$) and a plane perpendicular to it ($I_{\perp}$). The fluorescent aptamer binding to the virus was detected through an increase in the fluorescence polarization calculated as $FP = (I_{||} - I_{\perp} \cdot G) / (I_{||} + I_{\perp} \cdot G)$, where G is an instrument specific correction factor that was determined according to the instructions of the instrument manufacturer by using 1nM fluorescein solution. FP experiments were performed in 96 well, flat bottom, black microtiter plates (CLS3694, Corning) blocked previously with Pierce Protein-Free (TBS) Blocking Buffer (37570, ThermoFisher Scientific) for 1 h. The sum of volumes was 60 µl and the fluorescently labelled aptamer concentration 0.5 nM in each well. The FP values were reported as the average of 10 consecutive measurements after the binding equilibrium was reached (up to 1 h), which was confirmed by no change in the measured fluorescence intensities.

RESULTS AND DISCUSSION

Selective fluorescent labelling of RSV particles

Selective fluorescent labelling of RSV can be most straightforwardly achieved by using a fluorescent dye conjugated to specific receptor which binds to a viral protein on the virus envelope. The use of aptamers, beside their robustness and easy conjugation with fluorescent dyes was also motivated by their monovalency. We expected that this will rule out virus aggregation during their selective labelling. Furthermore, the ca. an order of magnitude smaller molecular weight of the aptamers (ca. 22 kDa) than that of conventional antibodies may led to larger surface coverage of virus particles and by that providing higher sensitivity in this type of application. We have previously selected and reported a large batch of aptamers for RSV with H8 aptamer exhibiting the best performance in proximity based luminescence assay of RSV.[24] However, as the suitability of aptamers may depend on the particular application, we have selected further aptamer candidates for this study. Their relative affinity for RSV was tested using competitive fluorescence polarization assay in which fluorescent aptamer candidates (B4, E6, E10, E11, H8) in a constant concentration of 0.5 nM competed for RSV (1.2×10^5 PFU/mL) with the unlabelled H8 aptamer. Fluorescence polarization is a homogeneous assay, i.e., does not require the immobilization of the aptamer and the separation of the free and virus bound aptamer. The fluorescence polarization scales inversely with the rate at which a fluorescent molecule rotates. Therefore, the binding of the aptamers to the large virus particles, which decreases significantly their rotational rate, can be easily followed through the increased FP.[26] The competitive FP format imposes further stringency to the binding process minimizing non-specific binding. The decrease in the fluorescence polarization upon increasing the unlabelled H8 aptamer concentration indicates the degree of displacement of the respective fluorescently labelled aptamers form the RSV, i.e., its relative affinity for RSV.

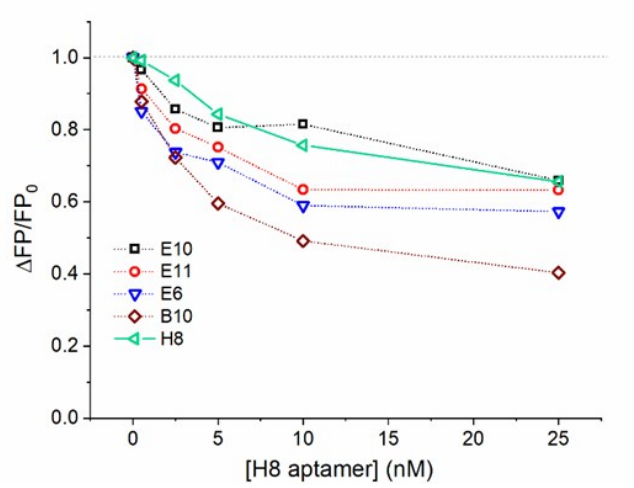

Fig. 1 Competitive homogeneous FP experiments performed by keeping the concentration of fluorescently labelled aptamers and that of the RSV virus constant at 0.5 nM and 1.2×10^5 PFU/mL, respectively, while varying the concentration of the unlabelled H8 aptamer. The curves were normalized with the FP value measured in the absence of the competing aptamer (FP_0).

As it can be seen in Fig. 1 aptamers H8 and E10 showed the highest relative affinity, followed closely by E6 and E11, with

B10 exhibiting significantly poorer performance. Based on this result H8 aptamer was used for most of the follow up measurements.

Fluorescence polarization experiments were carried out in the support of the selective labelling of the RSV virus. Human rhinovirus a likely coexisting pathogen in the RSV containing swab throat samples was used for this purpose and both virus formulations were incubated with the AlexaFluor488-H8 aptamer. At low virus concentrations (<10^6 PFU/mL) no association with the HRV could be observed while the binding to the RSV was detected at almost two orders of magnitude lower concentrations (Fig. 2A).

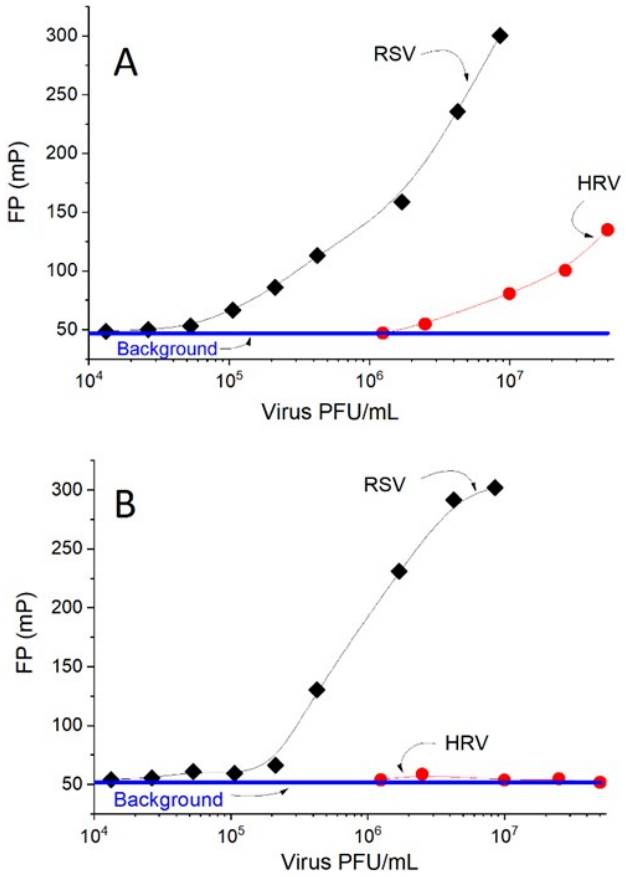

Fig. 2 Binding of AlexaFluor488-H8 aptamer (0.5 nM) to RSV and HRV in the absence (A) and in the presence (B) of randomDNA (10 nM) followed by FP.

It is likely that the significant aptamer binding at higher HRV concentrations is due to non-specific electrostatic interaction[27, 28] between the negatively charged aptamer and positively charged target domains. This is likely to occur as the homogeneous FP assay lacks of a stringent washing step that would disrupt no-specific interactions. If this scenario applies, adding an unlabelled random sequence DNA in sufficiently large concentration should displace, by competitive action, the aptamer from the HRV. We found that already a 10-fold excess (5 nM) random DNA background confirms this hypothesis, i.e. no HRV-aptamer complexes could be detected, while the fluorescent labelling of RSV was barely affected (Fig. 2B).

Sizing and counting of fluorescently labelled RSV particles

First the RSV virus formulations were investigated in the light scattering mode by NTA to assess the total number of particles. As expected, we found a rather broad size distribution, from ca. 40 nm to 1500 nm equivalent diameter (Fig. S1) with a total concentration of (2.4±0.19) × 10^{11} particles/mL (for the stock solution). The largest fraction of the detected particles fallen in the 100-200 nm range and tailed towards larger sizes (Fig. S1), however, this formulation may still include cell debris and other membrane or molecular aggregates. To reveal RSV viruses among these by selective fluorescent labelling we used H8 aptamer that we found earlier to possess the highest affinity to attachment glycoprotein (G) of the RSV. [24] The RSV sample (10x diluted stock solution) was incubated for 1 h with 625-fold excess of the aptamer (25 nM) with respect to the total particle concentration and the counting was performed in fluorescence mode. To avoid photobleaching the labelled virus formulations were flown continuously through the sensing zone to reduce their residence in the laser beam. It should be stressed that in contrast to the nanoparticle tracking analysis of fluorescent particles with "whole volume fluorescence" (e.g. fluorescent polymer beads) in our case only the surface of the virus particles is fluorescently labelled. The challenge is further increased by the fact that after labelling the free fluorescent aptamers are not separated from the virus particles. Such a separation-free detection clearly ads to the convenience of the method as a separation may affect both the size and concentration of the virus samples.[29] Since the size of the free fluorescent aptamer is much smaller than the lower detection limit of NTA in terms of size (~40 nm for these type of particles) they cannot be detected as separate fluorescent entities, but only as an increase in the fluorescent background. In contrast, we expected a significantly higher local concentration of the fluorescent aptamers binding to the RSV surface than that of the free aptamer concentration (Fig. S2 B, C). While accurate surface densities of glycoprotein G were not reported if considering a 100 nm diameter virus particle and only 100 aptamers per virus that would amount to a local concentration of fluorescent aptamers of ca. 320 nM, which is already more than an order of magnitude larger than that of the free aptamer. Indeed, while the unlabelled virus gave no fluorescence signal, the fluorescently labelled formulation provided clearly detectable fluorescent particles, i.e., (5.8±0.15) × 10^9 particles/mL (for the stock solution). This count however is significantly lower than measured in light scattering mode. To rule out that this lower number of fluorescent particles is caused by any deficiency of the aptamer binding to the G protein or lack of G proteins on some of the viral particles as suggested earlier,[19] the same experiment was repeated using fluorescent polyclonal antibodies specific to all RSV viral antigens. The size distribution histograms for both aptamer- and polyclonal antibody-based fluorescent labeling of virus particles was comfortingly identical (Fig. 3A).

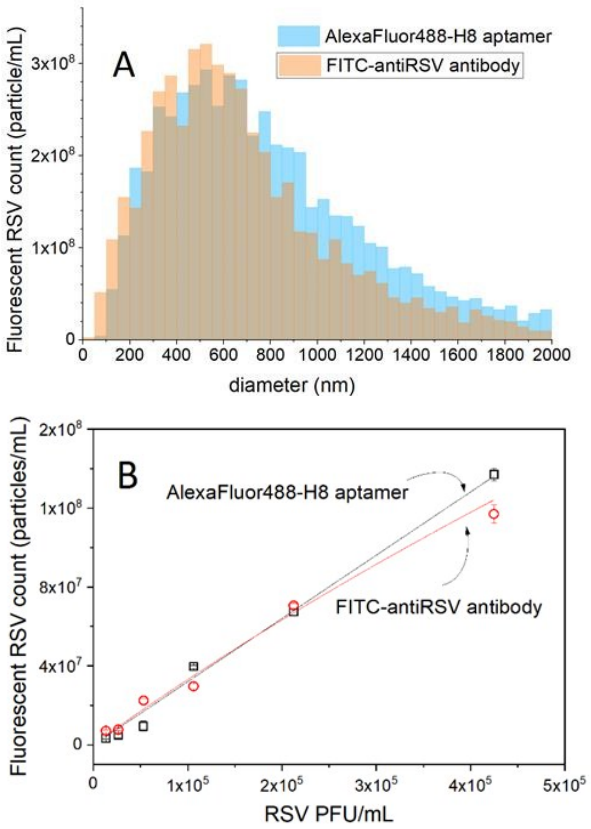

Fig. 3. (A) Size distribution of RSV viruses detected by NTA in fluorescent mode after labelling with fluorescent H8 aptamer and polyclonal RSV antibody. (B) NTA determined fluorescent RSV concentrations upon dilution of the RSV formulation.

Owing to the very large heterogeneity of RSV in terms of size and packing density of glycoproteins[19] it is difficult to estimate the number of G-proteins that need to be saturated by the fluorescent labeled aptamers. Increasing the aptamer concentration for G-protein saturation is not a reasonable option because it also elevates the fluorescent background that makes the fluorescent RSV particle detection difficult. However, by diluting the virus formulation a close to linear relationship was obtained between the number of detected virus particles and the viral concentration expressed in PFU/mL. At the highest dilution the aptamer is ~3.2×10^6 -fold excess in respect of the virus particles, thus the obtained linear relationship suggest that sufficient aptamer is available throughout the studied concentration range for the fluorescence visualization of the virus particles. The number of polyclonal antibody - and aptamer-labeled virus particles was found to be in excellent agreement, with the aptamer prevailing in terms of larger linear range at higher virus concentrations (Fig. 3B).

Thus after we ruled out contingent deficiencies of the aptamer binding and virus labelling the most likely explanation for the much lower particle count in fluorescence than in light scattering remains that the RSV preparations even after the purification steps contain a large quantity of cell debris. This assumption is also supported by the much smaller concentration of the infectious particles (PFUe) than the total RSV particles given by the fluorescent counting providing a particle-to-PFU ratio of 3200. These findings show clearly the utility and importance of the selective virus counting methodology proposed here in terms of virus standardization and characterization.

Detection of RSV in throat swab samples

To investigate the feasibility of the selective detection of RSV in clinically relevant matrices, throat swab samples collected from healthy individuals were used. First, it was demonstrated that the throat swab sample without the virus spiking does not contain any detectable fluorescent particles and does not affect the fluorescence of the Alexa488 labelled aptamer (Fig. S3). Next the 10-fold diluted throat swab samples were spiked with various concentrations of RSV. These samples were incubated with H8, B10 and E10 aptamers to investigate the influence of their relative affinity on the fluorescent RSV count. The results of the fluorescent NTA measurements performed on throat swab samples were compared with RSV samples formulated solely in PBS (Fig. 4A). We found a close to linear dependence between the fluorescent RSV count and the virus concentration for both PBS and throat swab samples with an insignificant effect of the choice of aptamers on the sensitivity. Although, the slope of the response in throat swab samples was ca. 1/3 of that of solely PBS-based formulations the result show clearly that RSV particles can be detected even in complex throat swab samples.

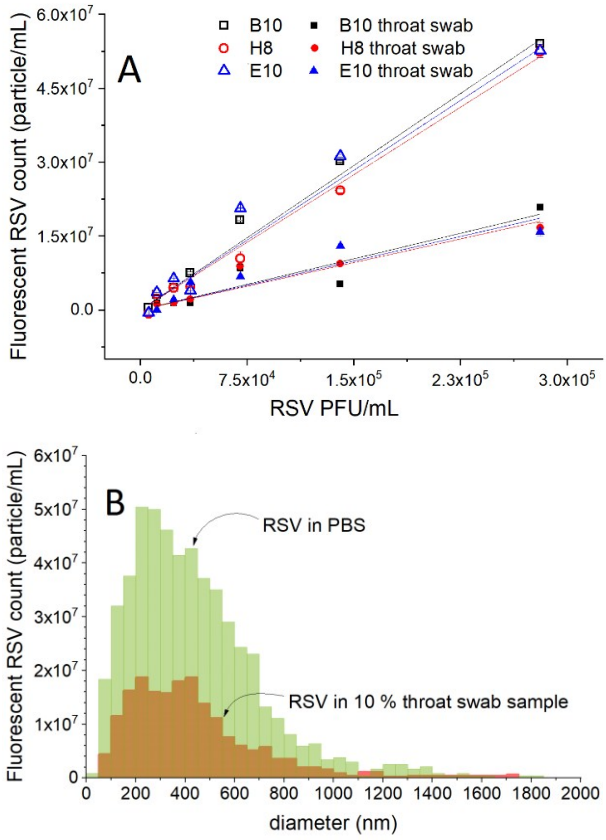

Fig. 4. Comparison of the fluorescent RSV count (A) and size distributions (B) detected after selective fluorescent labelling using different aptamers (25 nM) in PBS formulated RSV and 10-fold diluted throat swab samples.

Of note, since this method is capable of detecting single RSV particles the limit of detection in terms of concentration is in fact solely determined by the analysis time, i.e., for smaller concentrations larger sample volumes need to be passed through the cell, but for this proof of concept study we limited the analysis time to max. 20 min.

There is no change in the size distribution of the RSV viruses detected in the two media (Fig. 4B), which rules out contingent aggregation or selective loss of a size fraction. Since the throat swab sample was found to not affect the fluorescence of the aptamers the most likely reason for the lower fluorescence RSV count is the competitive displacement of the aptamers by constituents of the sample matrix, in particular the DNA background present in physiological samples. This assumption seems to be confirmed by fluorescence polarization assays in which different DNA backgrounds were established using salmon sperm DNA and the increasing of the DNA concentration led to decreasing FP values, i.e., removal of the fluorescent aptamers from RSV (Fig. S4). The lower number of aptamers that bind to a virus particle as result of competitive action of the sample matrix may reduce the number of detectable RSV particles, which could explain the sensitivity discrepancy of RSV determination in "pure" formulations and throat swab sample. However, even at DNA concentrations as high as 4 µg/mL the aptamer could not be fully displaced from the RSV indicating clinical applicability of the presented method.

In terms of virus counting the matrix effect of the throat swab samples clearly results in a negative bias. Therefore, while fluorescent nanoparticle tracking analysis is an absolute method and requires no calibration standards its direct use for such sample matrices makes the quantitation of RSV to be associated with a high uncertainty. This problem can be circumvented if the matrix effect on the RSV count is determined by standard addition, i.e., after the fluorescent RSV count is determined in the throat swab sample, the sample is spiked with RSV standards of known concentration. The ratio of the detected and nominal concentration of the RSV standard can be used as a correction factor to adjust the RSV concentration determined in throat swab samples. Given the variability of the throat swab samples among individuals this procedure is best to be applied for each individual throat swab sample. Table 1. demonstrates that using this standard addition technique the error in the quantification of RSV in throat swab samples can be reduced to ca. 25 %.

Table 1. Determination of virus counts in throat swab sampled with standard addition. The RSV particles were labelled with fluorescent H8 aptamer (25 nM) by incubation for 1 h.

RSV count (particle/mL)		Recovery (%)
Spiked	Measured	
5.53×10^7	5.74×10^7 (± 5.62×10^6)	103.8
8.43×10^7	6.37×10^7 (± 7.84×10^6)	75.6

Conclusions

View Article Online
DOI: 10.1039/C8NR01310A

In summary, here we show that single RSV particle detection is feasible by fluorescent nanoparticle tracking analysis following their selective labelling with fluorescent aptamers. Given the size discrimination capability of the method, the detection of fluorescently labelled RSV could be achieved even without separating the labelled virus from the free fluorescent aptamer. Thus this calibration-free counting and sizing method with little sample preparation is expected to be very appealing for virologist in terms of virus standardization. Moreover, given the single species detection ability of the proposed methodology, the selective detection of RSV was straightforward even in clinically relevant complex samples, such as diluted throat swab samples. However, the quantification in case of throat swab samples is complicated by a matrix effect (most likely a competitive effect) that results in a reduction of the fluorescent RSV count. We could circumvent this problem by correcting for the matrix effect using standard addition, but we foresee other possibilities in terms of improved receptor design. The very promising results for RSV, which is a difficult target, owing to its heterogeneity and variability in size and shape, suggest that the methodology may be generally applicable for viruses larger than ca. 80-100 nm. Certainly, the application of this method requires a sufficiently low background fluorescence of the sample matrix for the detection of the virus particles. However, this may be addressed by using fluorophores and spectral ranges that minimizes the autofluorescence of the sample.

Conflicts of interest

The authors declare no conflicts of interest.

Acknowledgements

This work was supported by the Lendület program of the Hungarian Academy of Sciences (LP2013-63) and ERA-Chemistry (OTKA NN117637). Marc Eleveld is gratefully acknowledged for the production of the RSV stocks.

References

1. C. H. van den Kieboom, S. L. van der Beek, T. Meszáros, R. E. Gyurcsányi, G. Ferwerda and M. I. de Jonge, *Trac-Trend Anal Chem*, 2015, 74, 58-67.
2. D. Raoult and P. Forterre, *Nat. Rev. Microbiol.*, 2008, 6, 315.
3. C. A. Rossi, B. J. Kearney, S. P. Olschner, P. L. Williams, C. G. Robinson, M. L. Heinrich, A. M. Zovanyi, M. F. Ingram, D. A. Norwood and R. J. Schoepp, *Viruses-Basel*, 2015, 7, 857-872.
4. P. Roingeard, *Mol. Biol. Cell Molecular*, 2008, 100, 491-501.
5. J. L. Huff, M. P. Lynch, S. Nettikadan, J. C. Johnson, S. Vengasandra and E. Henderson, *J. Biomol. Screening*, 2004, 9, 491-497.
6. S. Faez, Y. Lahini, S. Weidlich, R. F. Garmann, K. Wondraczek, M. Zeisberger, M. A. Schmidt, M. Orrit and V. N. Manoharan, *Acs Nano*, 2015, 9, 12349-12357.
7. I. Makra, P. Terejánszky and R. E. Gyurcsányi, *Methodsx*, 2015, 2, 91-99.

View Article Online
DOI: 10.1039/C8NR01310A

8. S. M. Scherr, G. G. Daaboul, J. Trueb, D. Sevenler, H. Fawcett, B. Goldberg, J. H. Connor and M. S. Unlu, *Acs Nano*, 2016, 10, 2827-2833.
9. B. Carr, A. Siupa, P. Hole, A. Malloy and C. Hannell, *Hum Gene Ther*, 2012, 23, A8-A9.
10. P. Kramberger, M. Ciringer, A. Strancar and M. Peterka, *Virol J*, 2012, 9.
11. P. Terejánszky, I. Makra, P. Fürjes and R. E. Gyurcsányi, *Anal Chem*, 2014, 86, 4688-4697.
12. Z. D. Harms, K. B. Mogensen, P. S. Nunes, K. M. Zhou, B. W. Hildenbrand, I. Mitra, Z. N. Tan, A. Zlotnick, J. P. Kutter and S. C. Jacobson, *Anal Chem*, 2011, 83, 9573-9578.
13. K. M. Zhou, L. C. Li, Z. N. Tan, A. Zlotnick and S. C. Jacobson, *J Am Chem Soc*, 2011, 133, 1618-1621.
14. J. D. Uram, K. Ke, A. J. Hunt and M. Mayer, *Abstr Pap Am Chem S*, 2007, 234.
15. B. Carr, A. Malloy and J. Warren, *IPT*, 2008, 38-40.
16. B. Carr, *Bio Tech International*, 2009, 21, 23-25.
17. D. Griffiths, P. Hole, J. Smith, A. Malloy and B. Carr, 2010.
18. O. Hayden, P. A. Lieberzeit, D. Blaas and F. L. Dickert, *Adv. Funct. Mater.*, 2006, 16, 1269-1278.
19. L. Liljeroos, M. A. Krzyzaniak, A. Helenius and S. J. Butcher, *PNAS*, 2013, 110, 11133-11138.
20. T. Bachi and C. Howe, *J. Virol.*, 1973, 12, 1173-1180.
21. L. S. Eiland, *JPPT*, 2009, 14, 75-85.
22. T. Popow-Kraupp and J. H. Aberle, *Open Microbiol. J.*, 2011, 5, 128-134.
23. M. Vissers, M. N. Habets, I. M. L. Ahout, J. Jans, M. I. de Jonge, D. A. Diavatopoulos and G. Ferwerda, *J. Visualized Exp.*, 2013, DOI: 10.3791/50766, 50766.
24. K. Percze, Z. Szakács, E. Scholz, J. András, Z. Szeitner, C. H. van den Kieboom, G. Ferwerda, M. I. de Jonge, R. E. Gyurcsányi and T. Meszáros, *Sci Rep-Uk*, 2017, 7.
25. M. Shafique, J. Wilschut and A. de Haan, *Vaccine*, 2012, 30, 597-606.
26. D. M. Jameson and W. H. Sawyer, in *Methods in Enzymology*, Academic Press, 1995, vol. 246, pp. 283-300.
27. G. Lautner, Z. Balogh, V. Bardoczy, T. Mészáros and R. E. Gyurcsányi, *Analyst*, 2010, 135, 918-926.
28. M. Menger, A. Yarman, J. Erdőssy, H. B. Yildiz, R. E. Gyurcsányi and F. W. Scheller, *Biosensors-Basel*, 2016, 6.
29. P. Terejánszky, I. Makra, A. Lukács and R. E. Gyurcsányi, *Electroanal*, 2015, 27, 595-601.

View Article Online
DOI: 10.1039/C8NR01310A

TOC ENTRY

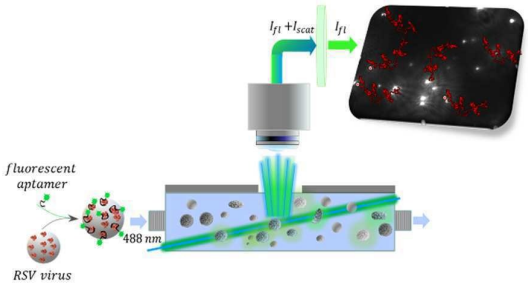

Selective labelling of virus particles with fluorescent aptamers enables their identification, sizing and counting at single particle level even in clinical samples by fluorescent nanoparticle tracking analysis.